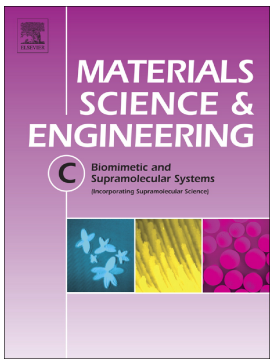

Silica nanoparticles with thermally activated delayed fluorescence for live cell imaging

Carina I.C. Crucho, João Avó, Roberto Nobuyasu, Sandra N. Pinto, Fábio Fernandes, João C. Lima, Mário N. Berberan-Santos, Fernando B. Dias

PII: S0928-4931(19)33106-6

DOI: https://doi.org/10.1016/j.msec.2019.110528

Reference: MSC 110528

To appear in: *Materials Science & Engineering C*

Received date: 22 August 2019

Revised date: 18 November 2019

Accepted date: 5 December 2019

Please cite this article as: C.I.C. Crucho, J. Avó, R. Nobuyasu, et al., Silica nanoparticles with thermally activated delayed fluorescence for live cell imaging, *Materials Science & Engineering C* (2019), https://doi.org/10.1016/j.msec.2019.110528

Silica Nanoparticles with Thermally Activated Delayed Fluorescence for Live Cell Imaging

Carina I.C. Crucho[a,‡], João Avó[a,‡,*], Roberto Nobuyasu[b,c], Sandra N. Pinto[a], Fábio Fernandes[a], João C. Lima[d], Mário N Berberan-Santos[a], Fernando B. Dias[b,*]

a. CQFM-IN and IBB-Institute for Bioengineering and Biosciences, Instituto Superior Técnico, Universidade de Lisboa, 1049-001 Lisboa, Portugal.
b. Physics Department, Durham University, South Road, Durham, DH1 3LE, UK
c. Instituto de Física e Química, Universidade Federal de Itajubá, Itajubá MG CEP 37500-903, Brazil
d. REQUIMTE, Departamento de Química, Faculdade de Ciências e Tecnologia, Universidade Nova de Lisboa, 2829-516 Caparica, Portugal.

Abstract

Thermally activated delayed fluorescence (TADF) has revolutionized the field of organic light emitting diodes owing to the possibility of harvesting non-emissive triplet states and converting them in emissive singlet states. This mechanism generates a long-lived delayed fluorescence component which can also be used in sensing oxygen concentration, measuring local temperature, or on imaging. Despite this strong potential, only recently TADF has emerged as a powerful tool to develop metal-free long-lived luminescent probes for imaging and sensing. The application of TADF molecules in aqueous and/or biological media requires specific structural features that allow complexation with biomolecules or enable emission in the aggregated state, in order to retain the delayed fluorescence that is characteristic of these compounds. Herein we demonstrate a facile method that maintains the optical properties of solvated dyes by dispersing TADF molecules in nanoparticles. TADF dye-doped silica nanoparticles are prepared using a modified fluorescein fluorophore. However, the strategy can be used with many other TADF dyes. The covalent grafting of the TADF emitter into the inorganic matrix effectively preserves and transfers the optical properties of the free dye into the luminescent nanomaterials. Importantly, the silica matrix is efficient in shielding the dye from solvent polarity effects and increases delayed fluorescence lifetime. The prepared nanoparticles are effectively internalized by human cells, even at low incubation concentrations, localizing primarily in the cytosol, enabling fluorescence microscopy imaging at low dye concentrations.

Keywords

Thermally-Activated Delayed Fluorescence; Confocal Microscopy; Silica Nanoparticles

Introduction

Fluorescence imaging and sensing methodologies have met a rapid growth in recent years and are increasingly gaining importance in detection and quantification of analytes due to their cost-effectiveness and notable sensitivity.[1,2] However, these techniques are affected by nonspecific and nonnegligible signals due to autofluorescence and light-scattering phenomena, which limit signal-to-noise ratio and resolution.[3] Time-gated acquisition using long-lived luminescence has been proven as an effective strategy to eliminate background and scattering interference. However, typical long-lived probes include phosphorescent transition-metal and lanthanide complexes that pose toxicity, stability and availability problems.[3] Therefore, developing metal-free emitters with long-lived luminescence is of great scientific and technological relevance. Small-molecule organic luminophores are particularly interesting candidates due to their established chemistry, scalability, and tunable physicochemical and biological properties. Amongst these, thermally activated delayed fluorescence (TADF) emitters have recently emerged as a powerful tool in the development of energy efficient organic light-emitting diodes (OLEDs).[4-6] These emitters display both conventional fluorescence - lifetime in the nanosecond range - and delayed fluorescence - lifetime ranging from micro- to milliseconds-, which result from the up-conversion of triplet states due to thermally-activated reversed intersystem crossing (RISC) from the triplet excited state (T_1) to the singlet excited state (S_1). Due to these two distinct emission lifetimes, TADF emitters are particularly interesting as optical probes, since they allow time-resolved and ratiometric detection with high signal-to-noise ratio without requiring transition-metal complexes.[7] Furthermore, the thermal activation of the RISC process grants these dyes the ability to optically measure temperature. However, despite these attractive properties, TADF emitters are so far rarely used in imaging and sensing applications in biological media, mainly due to their poor solubility and weak performance in water. In fact, TADF molecules rarely show strong luminescence in polar medium due to their charge transfer properties.[6] To overcome these limitations, several strategies have been recently tested.[7-12] For example, the complexation of TADF emitters with biomacromolecules[7] protects the dye from oxygen quenching, enhances the delayed emission and enables cell penetration. However, this approach relies on specific host-guest interactions and cannot be generalized to most TADF molecules. The precipitation of dyes into hydrophobic aggregates[8-10] has also been shown as a viable approach to achieve TADF emission in aqueous media, but the addition of amphiphilic agents or charged moieties is required to achieve cell penetration for imaging studies. Furthermore, this strategy can only be applied in TADF dyes that do not undergo self-quenching at high concentration or in the aggregated state and display aggregation-induced emission (AIE). Although several reported dyes display AIE, this phenomenon usually results in a change in the emission wavelength to lower energies, and is often accompanied by low quantum efficiencies and a decrease in delayed emission lifetime.[8-11] The most generalizable approach thus far proved to be the inclusion of native TADF emitters in vesicle-like structures of modified lipids, resulting in optically stable and oxygen-quenching resistant probes.[11-13] Nonetheless, this approach did not result in long delayed emission lifetimes that are desirable for time-resolved imaging. Therefore, methodologies that allow the detection of TADF in aqueous media and preserve the optical properties of the pristine emitter are desirable for time-resolved optical imaging and sensing.

Herein, we describe a method for the preparation of doped silica-based nanoparticles that exhibit TADF with long lifetime in aqueous media. This approach has been extensively applied

to conventional fluorescent dyes allowing their application in optical imaging and sensing by increasing their biocompatibility, enhancing emission and/or circumventing solubility problems,[14-16] but to the best of our knowledge has never been successfully used with TADF emitters. Silica was selected due to its proven good dye encapsulation and stabilization and biocompatibility in live cell fluorescence imaging.[17-19]

Experimental

Materials and Synthesis

Tetraethyl orthosilicate (TEOS, >99%), (3-aminopropyl) triethoxysilane (APTES), acetophenone, 4'-acetyl-benzoic acid, thionyl chloride and aqueous ammonium hydroxide (28 wt %; NH_4OH) were purchased from Sigma Aldrich. 2,7–dichlorofluorescein, hexamethylenetetramine and piperidine were purchased from TCI Europe. 1,3,5-trioxane was purchased from Fluka. 2-[methoxy(polyethylene)$_{9-12}$propyl]trimethoxysilane was purchased from Fluorochem. Absolute ethanol (EtOH) was purchased from Fisher Chemical. Deionized water purified using a Millipore Milli-Q system to a resistivity of 18.2 MΩ was used throughout the experiments unless otherwise stated. Argon (Ar) gas (Alphagaz 1, 99,999%) was purchased from Air Liquid. Reagents and solvents used in synthesis were all analytical grade. All the reactions were carried out in dry conditions under inert atmosphere. Solvents were degassed by standing with 4 Å molecular sieves for 48 hours.[20]

NMR Spectroscopy

^1H and ^{13}C NMR spectra were recorded at 400 MHz and 100 MHz respectively using a Bruker Avance III 400 spectrometer (Bruker BioSpin GmbH, Rheinstetten, Germany) in $CDCl_3$, DMSO-d_6 or D_2O, referenced to the solvent for both proton and carbon spectra.

Electron Microscopy

Scanning Electron Microscopy (SEM) images were obtained for vacuum dried nanoparticles deposited in silicon wafer substrate and coated with gold layer (5 nm thickness) with an acceleration voltage of 2 kV and aperture size of 30 µm. The size distribution was determined by measuring a minimum of 100 individual particles.

Transmission Electron Microscopy (TEM) images were obtained with a Hitachi 8100 electron microscope operating at 200 kV and 20µA. The SiNPs samples were dispersed in ethanol, sonicated and drop-casted onto Formvar-coated copper grids. The dry nanoparticle size was estimated by measuring the average diameter of 100 nanoparticles by using ImageJ software.

Optical Spectroscopy

Absorption and reflectance spectra were collected using a Shimadzu UV-3600 double beam spectrophotometer. Reflectance spectra were obtained for silica nanoparticles dispersed in $BaSO_4$. Emission spectra were collected in a Jobin Yvon Fluorolog fluorescence spectrometer, respectively. Emission is independent of excitation wavelength. The luminescence temperature dependence measurements were acquired using a model liquid nitrogen cryostat (Janis Research). Fluorescence decays of dyes were measured by the single-photon timing

method using nanoLED (IBH) excitation at 373 nm, with 500 ps pulse width. The electronic start pulses are shaped in a constant fraction discriminator (Canberra 2126) and directed to a time to amplitude converter (TAC, Canberra 2145). Emission wavelength (450 nm) is selected by a monochromator (Oriel 77250) imaged in a fast photomultiplier (9814B Electron Tubes Inc.), the PM signal is shaped as before and delayed before entering the TAC as stop pulses. The analogue TAC signals are digitized (ADC, ND582) and stored in a PC. For luminescent nanoparticles, fluorescence decays were measured by the single-photon timing method with laser excitation (365 nm) and emission at 550-620 nm. The setup consisted of a diode-pumped solid state (DPSS) continuous wave green Nd:YVO4laser (Millennia Xs, Spectra Physics) that pumped a mode locked Ti:sapphire laser (Tsunami, Spectra Physics, with tuning range 700–1000 nm, output pulses of 100 fs, and 80 MHz repetition rate that can be reduced down to 4 MHz by a pulse picker) or mode locked DPSS Nd:YVO4green laser (Vanguard 2000-HM532,Spectra Physics) synchronously pumping two cavity dumped dye lasers (701, Coherent, delivering 3–4 ps pulses of about 40 nJ/pulse at 3.4 MHz) working with rhodamine 6G and DCM. Intensity decay measurements were made by an alternating collection of impulses and decays with the emission polarizer set at the magic angle position. Impulses were recorded slightly away from the excitation wavelength with a scattering suspension, thus defining the instrument response function (IRF). Particle samples were prepared either as suspensions in solvent (0.1-0.5 % w/v) or immobilized in quartz plates using zeonex (20% in toluene) as binder.

Temperature dependent time-resolved emission spectra were focused onto a spectrograph and detected on a sensitive gated iCCD camera (Stanford Computer Optics) with sub-nanosecond resolution. Solutions were prepared with concentrations in the 10^{-5}-10^{-4} M range in different solvents, and samples were degassed using 5 freeze-pump-thaw cycles or bubbling Argon for 1 hour. Films for optical characterization were prepared in zeonex or poly(vinylalcohol) matrix by drop-casting onto a quartz substrate with an emitter concentration of 1% (w/w). Prompt fluorescence quantum yields (φ_{PF}) were determined using the standard method for free dye (vs rhodamine B), and with an integrating sphere for luminescent nanomaterials. Delayed fluorescence quantum yields (φ_{DF}) were determined in two different ways depending on the degree of oxygen quenching. In systems where the delayed emission was completely quenched by oxygen, φ_{DF} was determined using φ_{PF} as internal reference and the ratio of integrated areas of luminescence spectra acquired with and without oxygen, as given by equation 1, where $I_{degassed}$ and $I_{aerated}$ are the integrated spectra on a wavelength scale:

$$\phi_{DF} = \phi_{PF}\left(\frac{I_{degassed}}{I_{aerated}} - 1\right) \quad (1)$$

Where air equilibrated samples at room temperature showed delayed emission, φ_F was determined in degassed conditions at ca. 80 K (LT) where only prompt fluorescence is observed, and 298 K (RT), where both prompt and delayed fluorescence are observed. φ_{DF} was estimated using the ratio of integrated spectra acquired at both temperatures, as given by equation 2:

$$\phi_{DF} = \phi_F\left(\frac{I_{LT}}{I_{RT}} - 1\right) \quad (2)$$

where I_{LT} and I_{RT} are the integrated spectra on a wavelength scale. Equation 2 is valid only if the variation of the radiative and internal conversion rates with temperature can be neglected, in this case the ϕ_{DF}/ϕ_{PF} ratio varies only due to the TADF contribution. To evaluate whether

this is a reasonable assumption in our case, the prompt-fluorescence lifetime, τ_{PF}, was measured at 80 K and 298 K. No significant variation was observed, confirming that ϕ_{PF} can be taken in a good approximation as temperature independent. A strong indication that any variation observed in ϕ_{DF}/ϕ_{PF} is mostly due to the variation on the TADF contribution with temperature is obtained from Fig. S10. The PF decay of compound 4 in PVA shows no variation with temperature, whereas the DF component shows a pronounced variation, decreasing at low temperatures. Delayed fluorescence decays were measured in a Jobin Yvon Fluorolog fluorescence spectrometer with a pulsed xenon lamp with full-width at half-maximum of 3 μs. Decays were collected with a minimum 100 μs delay to remove any interference from the lamp.

Triplet formation quantum yields were determined using the singlet depletion method with benzophenone as standard (ε_T = 5750 $M^{-1}cm^{-1}$, Φ_T =1) with a flash photolysis setup composed of a LKS 60 ns laser photolysis spectrometer from Applied Photophysics, with a Brilliant Q-Switch Nd:YAG laser from Quantel, using the third harmonics (λ_{ex} = 355 nm, laser pulse half-width equal to 6 ns). First-order kinetics were observed for the decay of the lowest triplet state (T–T annihilation was prevented by the low excitation energy and/or low optical density at excitation wavelength, $A_{355nm} \leq 0.1$).

The transient spectra were obtained with the same apparatus by monitoring the optical density change at intervals of 10 nm over the 300–600 nm range and averaging at least 32 decays at each wavelength.

Dynamic Light Spectroscopy (DLS) was carried out on a Horiba nanoPartica SZ-100V2 Nanoparticle Analyzer. Nanomaterials were suspended in water (1 mg/mL) and the analysed samples were prepared by diluting the stock suspensions (1:100). Measurements were carried out at 90° scattering angle on quartz cuvettes at 25 °C. All tests were run six times for 30 seconds and the average values were presented and particle size was calculated by fitting the correlation curves using solver mathematical software from the Stokes-Einstein equation.

ζ-potential values were determined by laser doppler electrophoresis technique (SZ-100 nanopartica, Horiba). The Smoluchowski approximation was applied. For each sample the mean value of three determinations was established.

Live cell imaging

HeLa cell line (European Collection of Authenticated Cell Cultures, ECACC) were cultured in DMEM (ThermoFisher Scientific) supplemented with 10% fetal bovine serum (FCS) (GIBCO) and 1% of penicillin-streptomycin (Sigma Chemical Co., St. Louis, MO) at the incubator with controlled temperature (37 ˚C), humidity and CO_2 levels (5%). For confocal and two-photon excitation microscopic studies, the cells were grown on Ibidi μ-Slide 8 well glass bottom with an initial density of 1×10^4 cells per well. After cell confluency reached ~70%, 6.25-100 μg/mL of SiNPs and PEG-SiNPs or 0.75-200 μM of **4** were added separately in two different sets of experiments and maintained/cultured for a period of 0.5-24 h. After the desired incubation time, cells were carefully washed with DPBS (Thermo Fisher Scientific) and labelled with WGA-Alexa Fluor 633 and Hoechst 33342 according with instructions of the supplier (Thermo Fisher Scientific, Plasma Membrane and Nuclear Labeling dyes). A final washing step with DPBS was

also included. The cells were imaged using a laser scanning confocal microscope (Leica TCS-SP5) equipped with a continuous Ar-ion, HeNe and a Ti:sapphire laser. Hoechst 33342 dye emission was collected from 400 to 500 nm, WGA – Alexa Fluor 633 emission was collected from 640 to 700 nm and nanoparticle emission was collected from 500 to 600 nm. A 63x (1.2 N.A.) water immersion objective was used in the experiments.

Quantification analysis was carried out using the ImageJ software (version 1.48, http://imagej.nih.gov/ij/). For each image, individual cells are selected using membrane staining with WGA-Alexa 633, and a mask is attributed to each cell. The total fluorescence signal in the nanoparticle channel (500-600 nm) was integrated for cells incubated with and without (autofluorescence) nanoparticles, in order to determine the concentration dependent intracellular nanoparticle fluorescence signal and the fraction of cells that exhibit nanoparticle internalization. Number of cells analyzed per condition > 40.

MTT Tetrazolium Assay

The effect of the synthesized NPs on cell metabolic activity was determined by MTT [3-(4,5-dimethylthiazol-2-yl-2,5-tetrazolium bromide)] assay previously described.[21] Briefly, HeLa cells were plated at a density of 2×10^4 cells per well into the 96-well plate and cultured for 24 h at 37 ˚C in 5% CO_2 atmosphere. Then, the synthesized NPs at different concentrations (0– 200 µg/mL) were added in duplicate and incubated for additional 24 h. After the incubation period, media was carefully replaced with 100 µl of fresh complete media without disturbing cell contents followed by addition of 20 µl of MTT solution (5 mg/ml) and incubated for 3-4 h. Finally, the formazan crystals formed in the wells were dissolved using 150 µl of MTT solvent and the absorbance was read at 590 nm using a microplate reader (bmg labtech 96 Spectrostar Nano).

Dye and Particle Synthesis

Dichlorofluorescein dialdehyde (**1**)

The synthesis of compound **1** was carried out using a modified procedure from literature.[22]

To a solution of dichlorofluorescein (5 g, 12.5 mmol) in trifluoroacetic acid (25 mL), urotropine (8.75 g, 62.5 mmol) was added. The solution was stirred at 90 °C for 16 hours. To the resulting slurry, acetic acid (120 mL) and water (80 mL) were added and the mixture was stirred at room temperature for 24 hours, after which a red solid precipitated. The solid was filtered off and washed with water (50 mL) three times. The solid (4.2 g, 73%) was dried under reduced pressure and was used in the subsequent reactions without further purification. For analytical purposes, the orange solid was recrystallized from dichloromethane/DMSO mixture.

^{1}H NMR (400 MHz, DMSO-d6) δ 10.71(s, 2H, Ar-C**H**O), 8.05 (d, J = 7.4 Hz, 1H, $C_{6'}$-**H**), 7.85 (t, J = 7.4 Hz, 1H, $C_{4'}$-**H**), 7.78 (t, J = 7.4 Hz, 1H, $C_{5'}$-**H**), 7.39 (d, J = 7.6 Hz, 1H, $C_{3'}$-**H**), 7.26 (s, 2H, C_1-**H** and C_8-**H**). EA calc. for ($C_{22}H_{10}Cl_2O_7\cdot0.3\ CH_2Cl_2$): C 55.49, H 2.21; found: C 55.87, H 2.35.

4-acetyl-*N*-(3-(triethoxysilyl)propyl)benzamide (**2**)

To a solution of 4-acetylbenzoic acid (2g, 12 mmol) in dry chloroform (30 mL), thionyl chloride (5 mL) was added dropwise. The solution was refluxed under reduced pressure while stirring for 16 hours. After cooling to room temperature, dichloromethane (100 mL) was added to the reaction mixture and the solution was washed with water (20 mL) until no gas evolution was observed. The organic phase was washed with aqueous 1% $NaHCO_3$ solution (2 x 50 mL) and brine (50 mL) and dried with anhydrous $MgSO_4$. The solvent was removed by rotatory evaporation to yield 1.8 g (81%) of 4-acetylbenzoyl chloride as a pale yellow liquid, which was used in subsequent reactions without further purification.

To 0.55 g (3 mmol) of 4-acetylbenzoyl chloride in dry dichloromethane (10 mL), a solution of diisopropylethyl amine (0.78 g, 6 mmol) and 3-(aminopropyl)triethoxysilane (0.66 g, 3 mmol) in dry dichloromethane (20 mL) was added dropwise at 0 ˚C. The mixture was stirred under inert atmosphere at room temperature for 8 hours. Dichloromethane (100 mL) was then added and the solution was washed with aqueous 5% HCl (3 x 30 mL) and brine (50 mL) and dried with $MgSO_4$. The solvent was removed by rotatory evaporation to yield 0.72 g (71%) of compound **2** as a colorless liquid.

^{1}H NMR (400 MHz, $CDCl_3$) δ (ppm): 8.02 (d, *J* = 8.0 Hz, 2H, C_2-**H** and C_6-**H**), 7.89 (d, *J* = 8.1 Hz, 2H, C_3-**H** and C_5-**H**), 6.68 (bs, 1H, CON**H**), 3.85 (q, *J* = 7.0 Hz, 6H, Si-O-C**H$_2$**-CH_3), 3.51 (q, *J* = 5.8 Hz, 2H, C**H$_2$**-CH_2-CH_2-Si), 2.66 (s, 3H, Ar-COC**H$_3$**), 1.80 (m, 2H, C**H$_2$**-CH_2-Si), 1.24 (t, *J* = 6.9 Hz, 9H, Si-O-CH_2-C**H$_3$**), 0.74 (t, *J* = 7.8 Hz, 2H, C**H$_2$**-Si). ^{13}C NMR (133 MHz, $CDCl_3$) δ (ppm): 139.9, 138.0, 129.1, 127.0, 56.2, 43.7, 27.1, 25.0, 18.0, 12.5. EA calc. for ($C_{18}H_{29}NO_5Si{\cdot}CHCl_3$): C 46.87, H 6.21, N 2.88; found: C .94, H 6.04, N 2.75.

4,5-di(4'-(*N*-3-(triethoxysilyl)propyl)amide)phenylprop-2-enone)-2,7-dichloro-fluorescein (**3**)

To a solution of compound **2** (0.23 g, 0.6 mmol) in dry ethanol (10 mL), compound **1** (0.1 g, 0.2 mmol) and dry piperidine (0.16 g, 2 mmol) were added. The reaction mixture was refluxed and stirred under inert atmosphere for 2 hours[a]. After cooling down to room temperature, the solvent was partially removed by rotatory evaporation and diethylether (50 mL) was added. The precipitate was filtered off, washed with diethyl ether (3x50 mL) and purified by column chromatography using ethanol/chloroform (2:8) as eluent[b]. Compound **3** was obtained as a dark-red solid (0.14 g, 60%).

^{1}H NMR (400 MHz, DMSO-d6) δ (ppm) 8.56 (d, J = 14.2 Hz, 2H, Ar-CH=C**H**), 8.47 (d, J = 14.2 Hz, 2H, Ar-C**H**=CH), 7.98 (bs, 1H, $C_{6'}$-**H**), 7.89 (d, J = 7.2 Hz, 4H, $C_{2''}$-**H** and $C_{6''}$-**H**), 7.74 (s, 2H, CON**H**), 7.66 (d, J = 7.2 Hz, 4H, $C_{3''}$-**H** and $C_{5''}$-**H**) 7.51 (bs, 3H, C3'-**H**, C4'-**H** and C5'-**H**), 7.29 (bs, 1H, $C_{3'}$-**H**), 6.99 (s, 2H, C_1-**H** and C_8-**H**), 3.69 (q, J = 6.4 Hz, 12H, Si-O-C**H$_2$**-CH_3), 3.22 (t, J = 7.0 Hz, 4H, C**H$_2$**-CH_2-CH_2-Si), 1.59 (m, 4H, C**H$_2$**-CH_2-Si), 1.07 (t, J = 6.4 Hz, 18H, Si-O-CH_2-C**H$_3$**), 0.55 (t, J = 8.5 Hz, 4H, C**H$_2$**-Si). ^{13}C NMR (400MHz, DMSO-d6) δ (ppm): 189.1, 173.1, 156.2, 142.2, 137.2, 133.0, 129.6, 128.9, 128.0, 120.5, 118.7, 114.7, 110.3, 109.7, 58.1, 56.4, 43.9, 25.3, 19.3, 18.7, 7.54. EA calc. for $C_{58}H_{64}Cl_2N_2O_{15}Si_2{\cdot}{\cdot}C_{12}H_{30}O_3$)[c]: C 59.16, H 3.67, N 3.00; found: C 59.65; H 3.81; N 2.85.

[a] After 2 hours the reaction is only partially complete. However, longer reaction times resulted in silane condensation, leading to the formation of an insoluble red solid.

[b] Ethanol was used in place of methanol in the eluent is necessary to prevent silane condensation during silica -gel column chromatography.

[c] Upon drying compound **3** undergoes rapid condensation through silane moieties, with consequent elimination of ethoxy groups.

4,5-di(phenylprop-2-enone)-2,7-dichloro-fluorescein (**4**)

The synthesis of compound **4** was carried out using a modified procedure from the literature.[22] To a solution of acetophenone (0.36 g, 3 mmol) in dry ethanol (50 mL), dry piperidine (0.26 g, 3 mmol) and compound **1** (0.55 g, 1.2 mmol) were added. The mixture was refluxed and stirred under inert atmosphere for 16 hours. After cooling to room temperature, the solvent was removed by rotatory evaporation to obtain a dark red viscous liquid. To this mixture, diethyl ether (200 mL) was added and a dark solid precipitated off. The solid was filtered off and washed with diethyl ether (3x100 mL). The crude product was purified by silica-gel column chromatography using methanol/chloroform (1:9) as eluent, to yield 0.15 g (30 %) of compound **4** as a red solid.

^{1}H NMR (400 MHz, DMSO-d6) δ (ppm) 8.77 (d, J = 15.0 Hz, 2H, Ar-CH=C**H**), 8.40 (d, J = 15.0 Hz, 2H, Ar-C**H**=CH), 8.20 (d, J = 7.3 Hz, 1H, $C_{6'}$-**H**), 7.92 (d, J = 8.0 Hz, 4H, $C_{2''}$-**H** and $C_{6''}$-**H**), 7.55 – 7.42 (m, 9H, $C_{3'}$-**H**, $C_{4'}$-**H**, $C_{5'}$-**H**, $C_{3''}$-**H**, $C_{4''}$-**H** and $C_{5''}$-**H**), 6.83 (s, 2H, C_1-**H** and C_8-**H**). ^{13}C NMR (400MHz, DMSO-d6) δ 190.2, 173.2, 172.5, 155.9, 139.1, 135.3, 134.0, 132.8, 131.2, 130.2, 129.2, 129.0, 128.4, 127.1, 121.7, 110.6, 109.3. EA calc. for $C_{38}H_{22}Cl_2O_7 \cdot CHCl_3$: C 59.99, H 2.97; found C 59.62, H 3.05.

Dye-doped silica nanoparticles (**SiNPs**)

Silica nanoparticles were prepared according to literature procedures, by a modified Stöber method.[23] At room temperature, water (9 mL), ethanol (83 mL) and aqueous ammonia solution (28 %, 1.5 mL) were mixed in a 250 mL polypropylene flask. The flask was submerged in an oil bath at 50 °C. When the reaction temperature reached a stable temperature of 44 °C, a mixture of TEOS (4.5 mL, 20 mmol) and compound **3** (3 mL, 5.5 mg/mL in ethanol) was added dropwise to the above solution and the reaction proceeded at 44 °C for 24 hours. Thereafter, the particles were collected by centrifugation (30 000 g, 15 min), and washed once with ethanol/water 1:1 and thrice with ethanol. The resultant pink pellet was dried in vacuum overnight to obtain dye-doped silica nanoparticles in powder form (1.11 g).

Dye-doped PEGylated silica nanoparticles (**PEG-SiNPs**)

PEG-modified SiNPs were prepared according to the previously described procedure. In brief, a mixture composed of water (2 mL), ethanol (18.4 mL) and aqueous ammonia solution (28 %, 0.33 mL) were mixed in a 250 mL polypropylene flask and allowed to reach a stable temperature of 44 °C. Separately, 0.65 mL of a 5.5 mg/mL ethanolic solution of compound **3**, were mixed with TEOS (1 mL, 4.4 mmol) and 2-[methoxy(polyethylene)$_{9\text{-}12}$propyl]trimethoxysilane (0.32 mL, 0.66 mmol). This mixture was added dropwise to the above solution and the reaction proceeded at 44 °C for 24 hours. The gel was centrifuged (10 000 rpm, 10 min) and then washed with ethanol three times, followed by drying in vacuum overnight. The presence of PEG attached on the silica was verified using nuclear magnetic resonance spectroscopy (NMR).[23] An incorporation of 0.564 mmol/g of particles were calculated by NMR with 1,3,5-trioxane as internal standard (singlet at δ = 5.18 ppm).

Results and Discussion

TADF-emitting silica nanoparticles (SiNPs), were prepared by chemical derivatization of a known emitter with silane moieties. A recently reported fluorescein derivative was selected for its known TADF emission properties and easily addressable chemistry that allows functionalization for nanoparticle doping (Scheme 1).[22]

Scheme 1 Synthetic pathway for the preparation of TADF emitting fluorescein derivatives

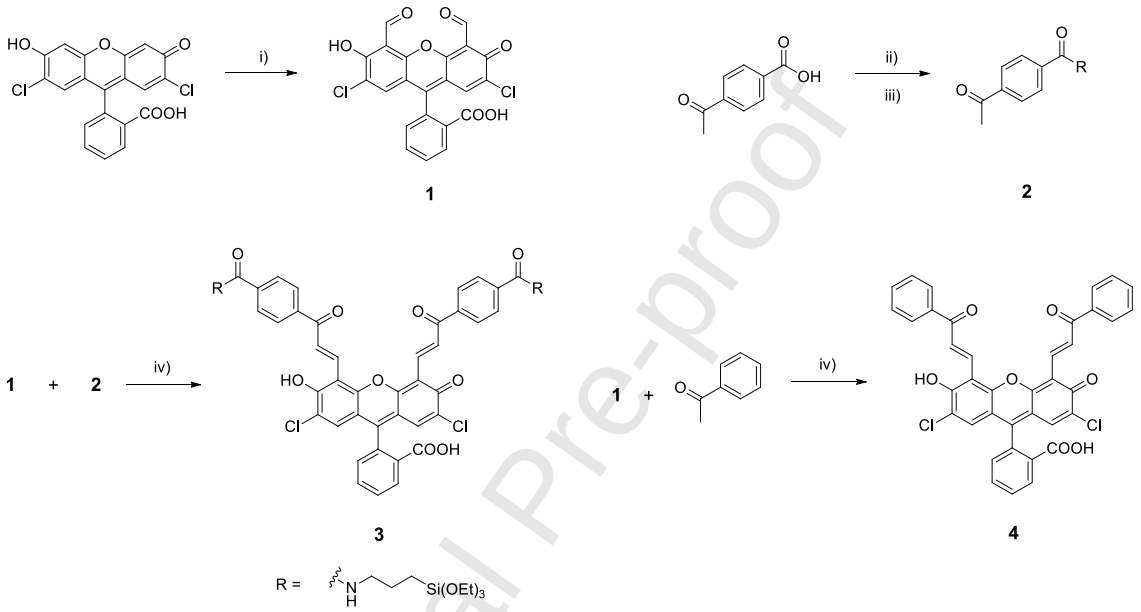

Conditions: i) hexamethylenetetramine, trifluoroacetic acid, acetic acid; ii) thionyl chloride, chloroform; iii) (3-aminopropyl)triethoxysilane, dichloromethane; iv) piperidine in ethanol

The synthesis of this dye (**3**) is achieved in three steps. Initially, 2,7-dichlorofluorescein is formylated via a Duff reaction. In parallel, a triethoxysilane moiety is appended to an acetophenone derivative. Finally, the acetophenone is then condensed via a Knœvenagel reaction. In order to compare the optical properties of SiNPs with those of the free dye and determine the effects of dye-grafting in the photophysics, a non-silanized analog (**4**) was also prepared using the same synthetic procedure.

SiNPs were prepared using a modified Stöber process from tetraethoxysilane and **3** in water.[23] Evident from TEM image analysis (Figure 1), silica nanospheres (Stöber) with ca. 35 nm in diameter were obtained.

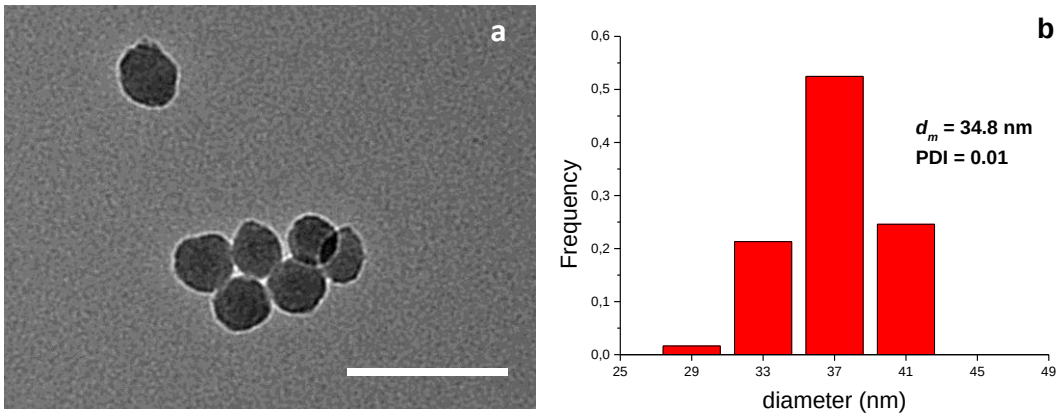

Figure 1 TEM image (a) and size distribution (b) of prepared SiNPs doped with compound **3**. (ø = 35 nm, scale bar = 100 nm)

The optical properties of the prepared SiNPs and compound **4** were characterized using steady-state and time-resolved absorption and emission spectroscopy. Figure 2 depicts the normalized emission spectra of the SiNPs in water and of **4** in water and ethanol, which evidence the effect of the silica matrix on the photophysical properties of the dye. While the emission maximum of compound **4** is centered at ca. 530 nm, consistent with the emission of phenylenone fluorescein derivatives in water,[22] the emission maxima of the prepared particles is shifted to lower energies, similar to the emission spectra of **4** in ethanol and other less polar organic solvents (Supplementary Material, Figure S6). Furthermore, the emission maximum centered at 585 nm for the SiNPs is consistent with a homogeneous dispersion of the dye in the silica matrix, as the aggregation shifts the emission to even longer wavelengths (ca. 660 nm, Supplementary Material, Figure S8). The contribution of an emission appearing at 530 nm as a shoulder in the SiNPs spectrum can be attributed to the outermost dyes that are in contact with water.

To evaluate the effect of dye-doping silica in the delayed emission properties, time-resolved emission spectra were collected. Since the delayed fluorescence of these fluorescein derivatives is not detectable in water,[7,22] the prompt and delayed fluorescence spectra of **4** were collected in ethanol for comparison. Figures 3a and 3b show the time-resolved spectra of the prepared SiNPs dispersed in water and compound **4** dissolved in ethanol, respectively. It is clear that, in both cases, the presence of oxygen in the sample greatly decreases the delayed component of the emission, demonstrating that the silica matrix of the SiNPs is permeable to gasses and is not effective at preventing oxygen quenching of excited triplet states. Nonetheless, grafting to the silica matrix significantly increases the delayed emission lifetime, as evidenced by the emission decays depicted in insets of Figure 3. Whereas compound **4** exhibits a delayed fluorescence lifetime of ca. 0.11 ms in ethanol, SiNPs suspended in water exhibit a lifetime ca. 10 times longer (τ_{DF} = 1.20 ms), similar to that of compound **4** in solid film (Supplementary Material, Figure S11).

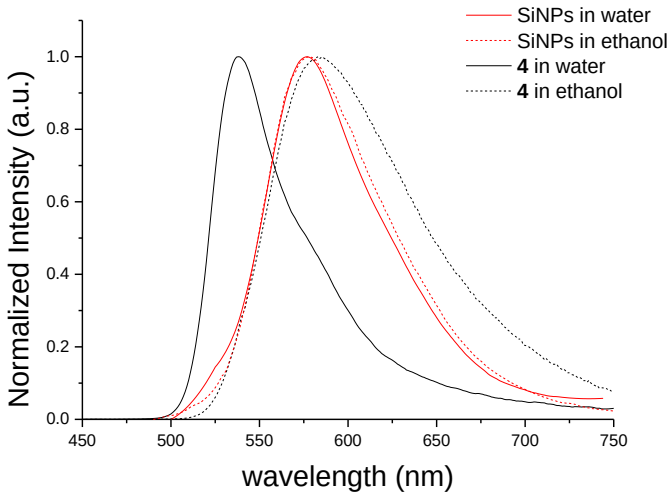

Figure 2 Normalized steady-state emission spectra of SiNPs (red lines) and compound **4** (black lines) in water and ethanol.

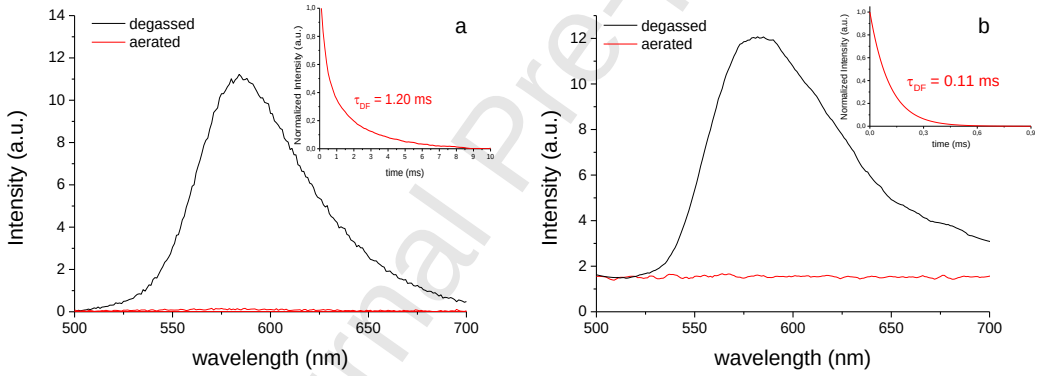

Figure 3 Time-resolved spectra of a) SiNP dispersed in water and b) compound **4** dissolved in ethanol. Delay = 0.1 ms, Integration = 2 ms. Insets show normalized emission decays in degassed conditions.

These results suggest that the grafting of the dye reduces the non-radiative decay pathway by restricting molecular vibrations, which is desirable for time-resolved imaging applications. Thus, this strategy effectively enables detection of TADF in aqueous media, where the SiNPs are suspended. Table 1 summarizes the effects of dye grafting in the photophysical properties, regarding prompt (φ_{PF}) and delayed (φ_{DF}) fluorescence quantum yields, lifetime (τ_{PF} and τ_{DF}), and emission maxima wavelength (λ_{em}). It is evidenced that doping silica nanoparticles has an overall positive effect on the emissive properties of this fluorescein derivative in aqueous media, with an increase in the photoluminescence quantum yield (PLQY) and τ_{DF}.

Table 1 Prompt and delayed fluorescence quantum yield (φ_{PF}, φ_{DF}), lifetime (τ_{PF}, τ_{DF}) and wavelength (λ_{PF}, λ_{DF}) of SiNPs and compound **4**.

	φ_{PF}	τ_{PF} (ns)	φ_{DF} [c]	τ_{DF} (ms)	λ_{PF} (nm)	λ_{DF} (nm)

SiNPs		0.06[a]	1.88	0.01	1.20	577	585
4	H_2O	0.02[b]	0.19	N/D	N/D	538	N/D
	EtOH	0.24[b]	2.48	0.04	0.11	581	582

a) determined using an Integrating Sphere; b) determined using the comparative method against fluorescein; c)determined from the ratio $\frac{I_{degassed}}{I_{aerated}}$

However, the PLQY of SiNPs is significantly lower than that of compound **4** in ethanol. This result can be attributed to the high polarity of the silica matrix, since the optical properties of **4** are affected by media polarity.[22] To test this hypothesis, we prepared luminescent nanoparticles using a modified silica source bearing small polyethyleneglycol (PEG) chain (Scheme 2). The TEM image depicted in Figure 4 shows that changing the silica source did not significantly change particle morphology but resulted in an increase in size (from 35 to 73 nm). In addition, dynamic light scattering (DLS) measurements show that the modified silica nanoparticles (PEG-SiNPs) increased the absolute value of the zeta-potential compared to the pristine silica counterparts (-84 mV vs 38 mV, Figure S24-25).

In principle, the presence of oligoether chains inside the silica matrix also lowers its polarity and enhances dye PLQY. Thus, the optical properties of PEG-SiNPs were investigated. Figure 5 depicts the steady state and time-resolved spectra of PEG-SiNPs in water, and Table 2 summarizes their PLQY and emission lifetime values.

Scheme 2 Chemical structure of oligoether-modified silica source

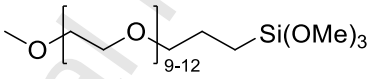

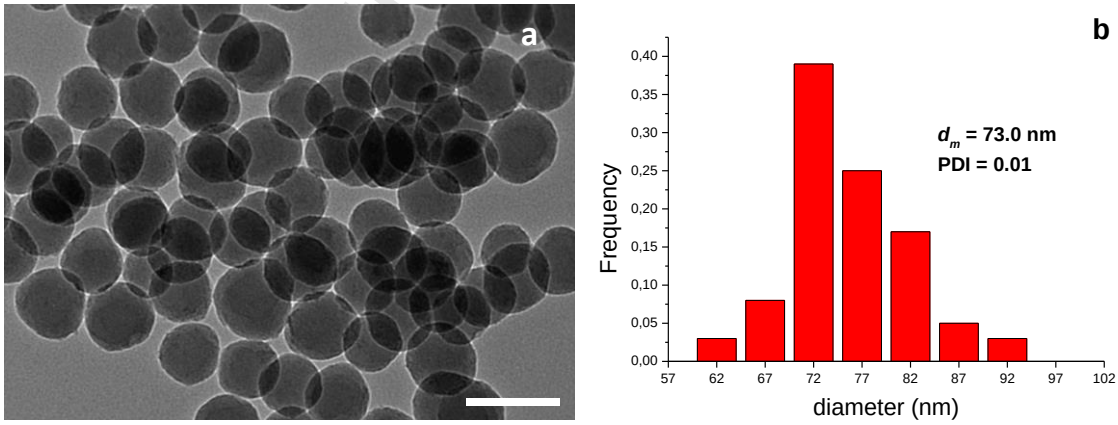

Figure 4 TEM image (a) and size distribution (b) of prepared PEG-SiNPs doped with compound **3**. (ø = 73 nm, scale bar = 100 nm)

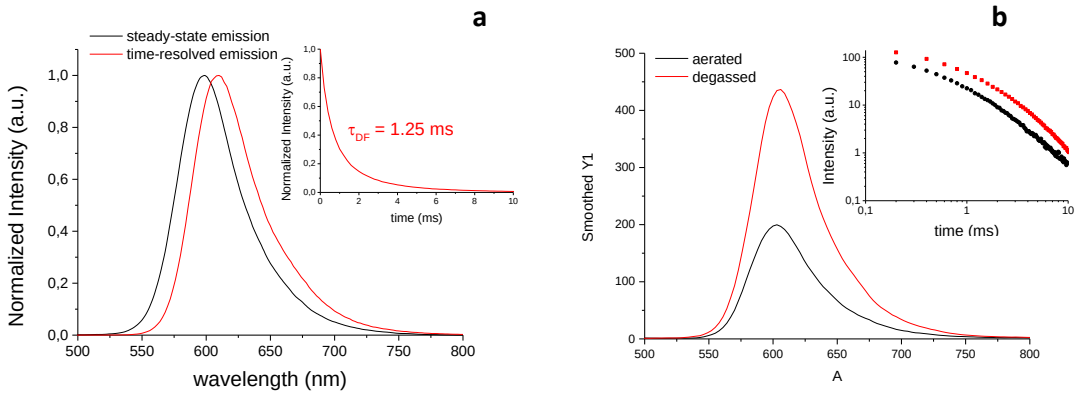

Figure 5 a) Steady-state (black line) and time-resolved (red line) emission spectra of PEG-SiNPs in water. Delay = 0.1 ms, Integration = 2 ms. Inset shows the delayed emission decay; b) time-resolved spectra collected before (black) and after (red) degassing. Delay = 0.1 ms, Integration = 2 ms. Inset shows the emission decay in both conditions.

Table 2 Prompt and delayed fluorescence quantum yield (φ_{PF}, φ_{DF}), lifetime (τ_{PF}, τ_{DF}) and wavelength (λ_{PF}, λ_{DF}) of PEG-SiNPs

	φ_{PF} [a]	τ_{PF} (ns)	φ_{DF} [b]	τ_{DF} (ms)	λ_{PF} (nm)	λ_{DF} (nm)
PEG-SiNPs	0.20	2.57	0.07	1.25	599	610

a) determined using an Integrating Sphere; b) determined from the ratio $\frac{I_{RT}}{I_{LT}}$

The data show that the modification of the silica matrix has a marked effect both in the PLQY of the grafted dye and its emission wavelength, which are consistent with a decrease in matrix polarity. Moreover, the PEGylated silica matrix prevents oxygen quenching and TADF is detected even without degassing (Figure 5b). Overall, these results show that the addition of the oligoether-modified siloxane in the preparation of PEG-SiNPs led to an improvement of their optical properties towards application in fluorescence imaging. Thus, to assess the applicability of the luminescent silica nanoparticles as optical probes, cytotoxicity and cell internalization were evaluated for immortalized human cervical cancer (HeLa) cells. Figure 6 shows that the cell viability, evaluated using the MTT assay, gradually decreases upon increasing concentration of silica nanoparticles. At concentrations above 25 µg/mL, PEG-SiNPs show less toxicity than their pristine silica counterparts. Confocal microscopy images were acquired for HeLa cell cultures incubated in the presence of SiNPs and PEG-SiNPs at concentrations of 6.25 - 100 µg/ml (Figures 7-9). The images evidence that the nanomaterials internalize after 24 hours of incubation and their emission is detectable inside the cells. Through selective staining of nuclei and membrane, it is shown that both pristine and PEGylated silica nanoparticles accumulate primarily in the cytosol. At incubation concentration of 100 µg/ml, corresponding to a cell viability of ca. 50%, images with excellent contrast are acquired for both SiNPs and PEG-SiNPs (Figure 7). Through the quantification of dye grafted

onto the nanoparticle matrix, a incubation concentration of 100 µg/ml corresponds to a dye concentration of 0.16 µM for SiNPs and 0.53 µM for PEG-SiNPs (Table S2), which is significantly lower than the concentration previously reported for compound **4** in fluorescence imaging (20 µM).[22]

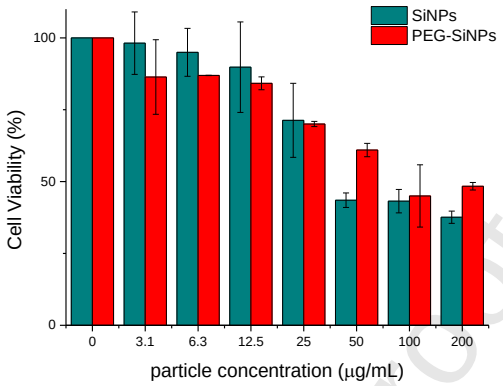

Figure 6 Effect of SiNPs and PEG-SiNPs on HeLa cell viability. HeLa were treated with various concentrations of SiNPs (blue) and PEG-SiNPs (red) (0-200 µg/mL) during 24h. HeLa cells viability was measured by the MTT assay. The percentages refer to relative cell viability represented as percentage of control. Incubation time = 24 hours.

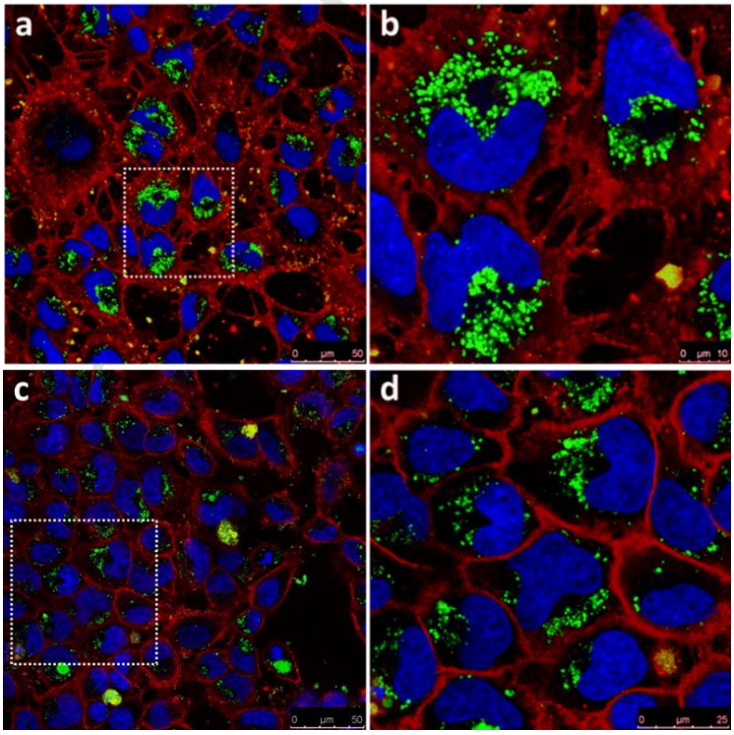

Figure 7 Confocal microscopy images of HeLa cells incubated for 24h in the presence of SiNPs (a and b) and PEG-SiNPs (c and d). Images show cell nuclei labelled with Hoechst 33342 (blue) and plasma membrane labelled with WGA-Alexa Fluor 633 (red). Fluorescence from TADF emitting nanoparticles is shown in green. The cells were incubated with NPs (100 µg/mL) for 24 hours at 37 °C.

At high cell viability conditions (>80%, 6.25 – 25 µg/mL) both types of nanomaterials also undergo efficient cell internalization, with measured fluorescence intensity proportional to concentration in incubation medium (Supplementary Material, Figure S27). When compared to the images obtained for 100 µg/mL, it is clearly evidenced that the decrease in nanoparticle concentration in the incubation medium leads to a significant decrease in the measured fluorescence (Figures 8 and 9). Nonetheless, for both pristine and modified silica nanopartides, luminescence in the cytosol is easily detected, with over 50% of cells exhibiting nanoparticle internalization, even for incubation concentrations as low as 6.25 µg/mL, for which cytotoxicity levels are very low (Supplementary Material, Figure S28). Compared to compound **4**, the grafting of the dye in pristine and modified silica improves its applicability in fluorescence microscopy, enabling internalization, improving optical properties and allowing its detection at significantly lower concentrations.[22]

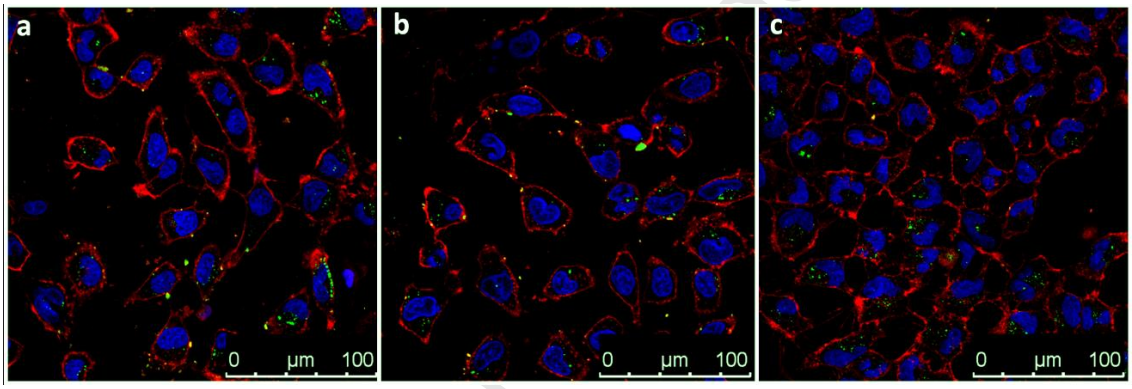

Figure 8 Confocal microscopy images of HeLa cells incubated for 24h in the presence of SiNPs at different concentrations: a) 25 µg/mL; b) 12.5 µg/mL; c) 6.25 µg/mL. Blue = cell nucleus labelled with Hoechst 33342; Red = Cell membrane labelled with WGA – Alexa Fluor 633; Green = TADF emitting nanoparticles. The cells were incubated with SiNPs for 24 hours at 37 °C.

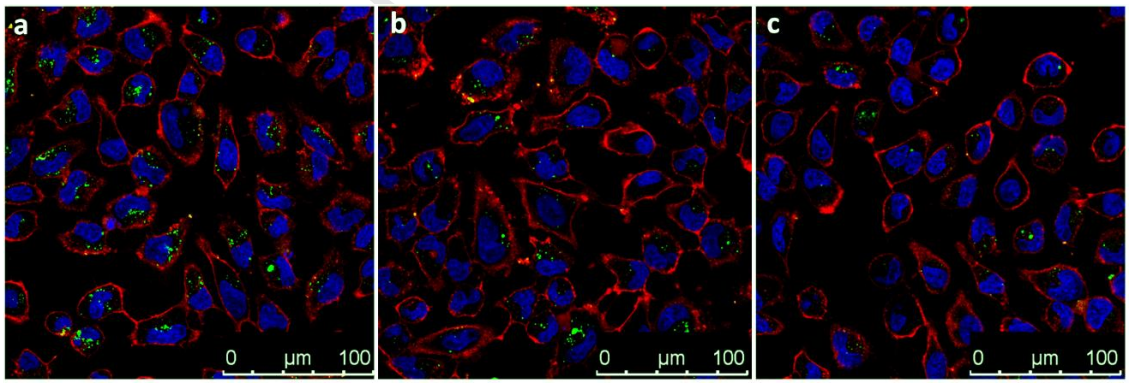

Figure 9 Confocal microscopy images of HeLa cells incubated for 24h in the presence of PEG-SiNPs at different concentrations: a) 25 µg/mL; b) 12.5 µg/mL; c) 6.25 µg/mL. Blue = cell nucleus labelled with Hoechst 33342; Red = Cell membrane labelled with WGA – Alexa Fluor 633; Green = TADF emitting nanoparticles. The cells were incubated with PEG-SiNPs for 24 hours at 37 °C.

Conclusions

In conclusion, a known TADF emitter with weak emission in water was used to dope water-dispersible silica nanoparticles with diameter below 100 nm. The dye-doping strategy proved successful in maintaining the optical properties of the dye in aqueous media without depending on host-guest complexation or aggregation induced emission phenomena. Furthermore, the delayed fluorescence lifetime increased over 10-fold upon inclusion in silica nanoparticles. The polarity of the nanoparticle matrix was tuned through the addition of a modified silane derivative, which resulted in a marked enhancement of the optical properties of the dye, leading to an increase in overall fluorescence quantum yield and enabling delayed fluorescence emission even in the presence of oxygen. Silica has been used extensively as a prime nanocarrier material for conventional fluorescent probes, and these results demonstrate its applicability also for developing TADF-emitting nanomaterials for time-resolved fluorescence microscopy imaging of live-cells. We expect that this strategy can be generalized to a wide variety of TADF emitters and, thus, pave the way for further development in time-resolved biological and medical imaging research applications.

Conflicts of Interest

There are no conflicts of interest to declare.

Acknowledgements

J. A. acknowledges FCT for funding under grant SFRH/BPD/120599/2016 and project PTDC/QUI-QFI/32007/2017. We also acknowledge Plataforma Portuguesa de Bioimagem (POCI-01-0145-FEDER-022122).

References

1 M. Gao, F. Yu, C. Lu, J. Choo, L. Chen, Chem. Soc. Rev. **2017**, 46, 2237-2271

2 P. Sarder, M. Dolonchampa, S. Achifelu, Bioconjugate Chem. **2015**, 26, 963-974.

3 Q. Zhao, C. Huang, F. Li, Chem. Soc. Rev. **2011**, 40, 2508-2524.

4 Y. Tao, K. Yuan, T. Chen, P. Xu, H. Li, R. Chen, C. Zheng, L. Zhang, W. Huang, Adv. Mater. **2014**, 26, 7931–7958.

5 Z. Yang, Z. Mao, Z. Xie, Y. Zhang, S. Liu, J. Zhao, J. Xu, Z. Chi, M. P. Aldred, Chem. Soc. Rev., **2017**, 46, 915-1016.

6 F. B. Dias, T. J. Penfold, A. P. Monkman, Methods Appl. Fluoresc. **2017**, 5, 012001.

7 X. Xiong, F. Song, J. Wang, Y. Zhang, Y. Xue, L. Sun, N. Jiang, P. Gao, L. Tian, X. Peng, J. Am. Chem. Soc. **2014**, 136, 9590-9597.

8 Z. Zhu, D. Tian, P. Gao, K. Wang, Y. Li, X. Shu, J. Zhu, Q. Zhao, J. Am. Chem. Soc. **2018**, 140, 17484-17491.

9 F. Ni, Z. Zhu, X. Tong, M. Xie, Q. Zhao, C. Zhong, Y. Zou, C. Yang, Chem. Sci. **2018**, 9, 6150-6155.

10 F. Ni, Z. Zhu, X. Tong, W. Zeng, K. An, D. Wei, S. Gong, Q. Zhao, X. Zhou, C. Yang, Adv. Sci. **2019**, 6, 1801729.

11 X. Luo, J. Meng, B. Li, A. Peng, Z. Tian, New J. Chem. **2019**, 43, 10735-10743.

12 T. Li, D. Yang, L. Zhai, S. Wang, B. Zhao, N. Fu, L. Wang, Y. Tao, W. Huang, Adv. Sci. **2017**, 4, 1600166.

13 Y. Tsuchiya, K. Ikesue, H. Nakanotani, C. Adachi, Chem. Commun. **2019**, 55, 5215-5218.

14 M. Montalti, L. Prodi, E. Rampazzo, N. Zaccheroni, Chem. Soc. Rev. **2014**, 43, 4243-4268.

15 J. Peng, J. Li, W. Xu, L. Wang, D. Su, C. L. Teoh, Y.-T. Chang, *Anal. Chem.* **2018**, 90, 1628-1634.

16 C. Zong, K. Ai, G. Zhang, H. Li, L. Lu, *Anal. Chem.* **2011**, 83, 3126-3132.

17 K. Wang, X. He, X. Yang, H. Shi, *Acc. Chem. Res.* **2013**, 46, 1367-1376

18 J. Malinge, C. Allain, A. Brosseau, P. Audebert, *Angew. Chem. Int. Ed.* **2012**, 51, 8534-8537

19 X. Song, F. Li, J. Ma, N. Jia, J. Xu, H. Shen, *J. Fluoresc.* **2011**, 21, 1205-1212

20 D.B.G. Williams, M. Lawton, *J. Org. Chem.* **2010**, 75, 8351-8354

21 N. Bernardes, A. R. Garizo, S. N. Pinto, B. Caniço, C. Pergigão, F. Fernandes, A. M. Fialho, *Cell Cycle*, **2017**, 17, 1649-1666

22 Y. Wu, F. Song, W. Luo, Z. Liu, B. Song, X. Peng, *ChemPhotoChem* **2017**, 1, 79-83.

23 C.I.C. Crucho, C. Baleizão, J. P. Farinha, *Anal. Chem*. **2017**, 89, 681-687.

Author Statement

The following is a list of contribution of each author to the manuscript entitled "Silica Nanoparticles with Thermally Activated Delayed Fluorescence for Live Cell Imaging", submitted to Materials Science and Engineering C, according to the Contributor Roles Taxonomy.

Carina I.C. Crucho: Methodology, Investigation, Writing

João Avó: Conceptualization, Investigation, Writing, Funding Acquisition

Roberto Nobuyasu: Investigation, Methodology

Sandra N. Pinto: Investigation, Methodology

Fábio Fernandes: Resources, Formal analysis, Validation

João C. Lima: Supervision, Validation, Resources

Mário N Berberan-Santos: Supervision, Validation, Resources

Fernando B. Dias: Validation, Writing, Funding Acquisition, Resources

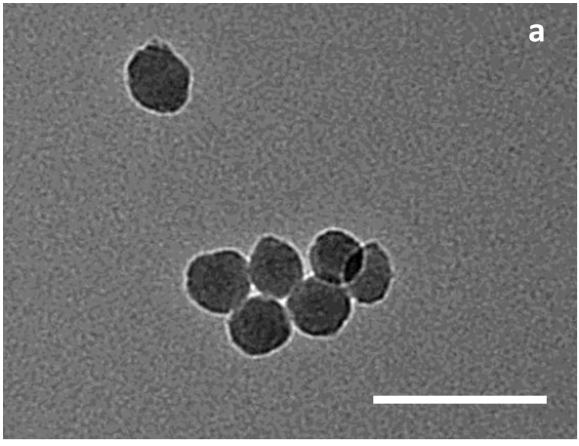
a

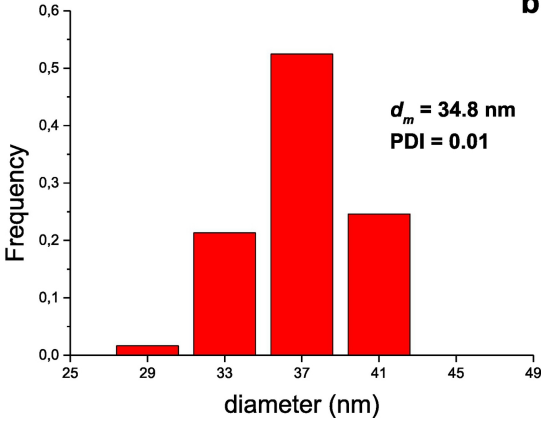
b
0,6
0,5
0,4
0,3
0,2
0,1
0,0
Frequency
d_m = 34.8 nm
PDI = 0.01
25
29
33
37
41
45
49
diameter (nm)

Figure 1

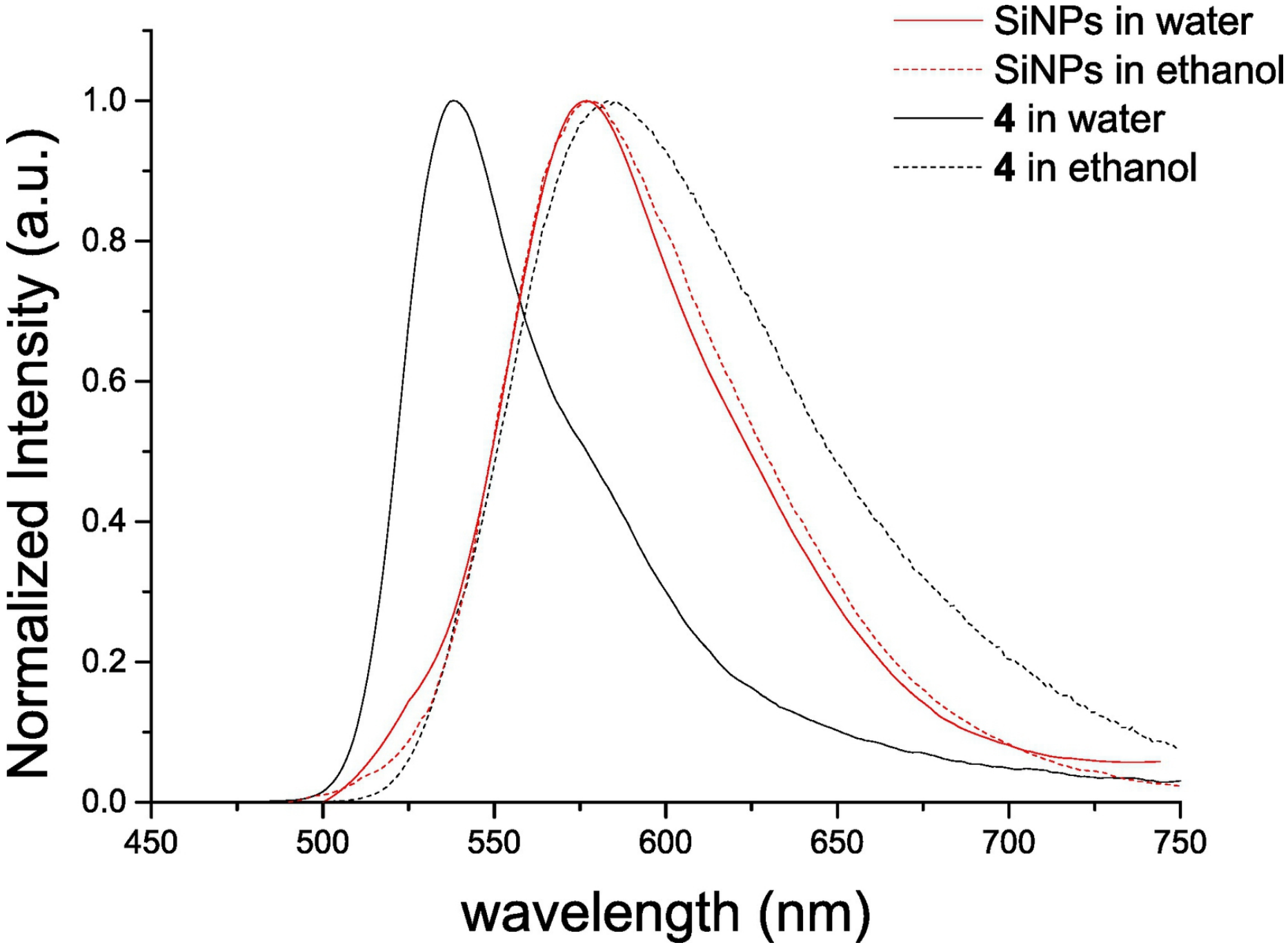
SiNPs in water
SiNPs in ethanol
4 in water
4 in ethanol
Normalized Intensity (a.u.)
1.0
0.8
0.6
0.4
0.2
0.0
450
500
550
600
650
700
750
wavelength (nm)

Figure 2

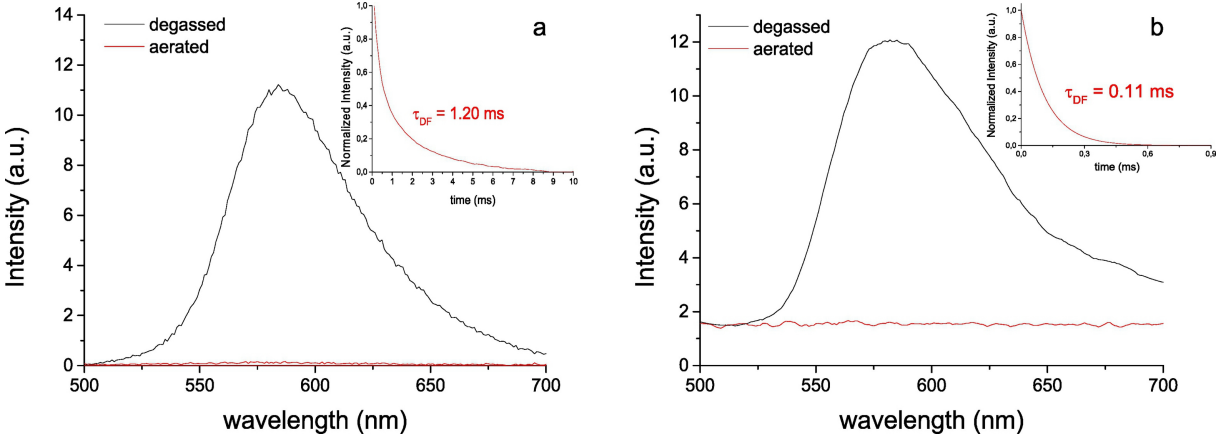
degassed
aerated
a
Intensity (a.u.)
wavelength (nm)
Normalized Intensity (a.u.)
time (ms)
τ_{DF} = 1.20 ms
b
τ_{DF} = 0.11 ms

Figure 3

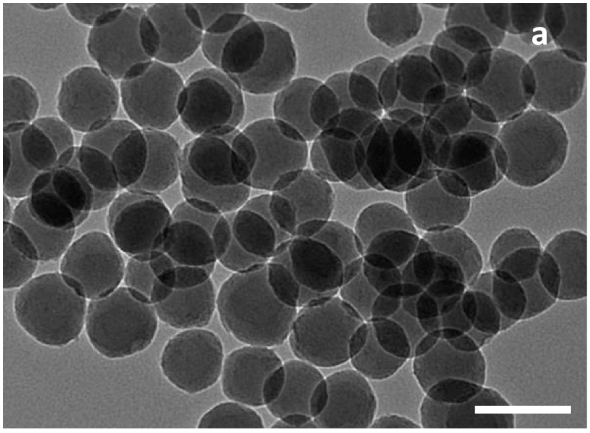
a

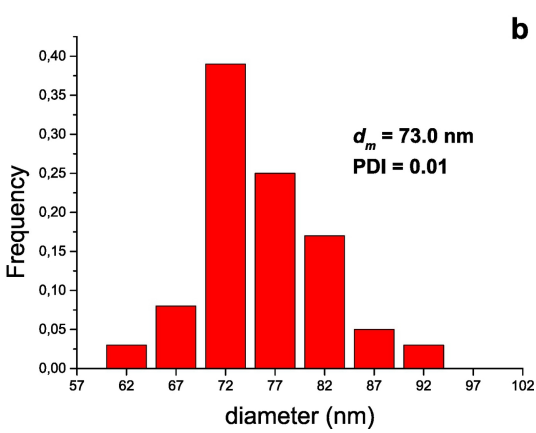
b
d_m = 73.0 nm
PDI = 0.01
Frequency
0,40
0,35
0,30
0,25
0,20
0,15
0,10
0,05
0,00
57
62
67
72
77
82
87
92
97
102
diameter (nm)

Figure 4

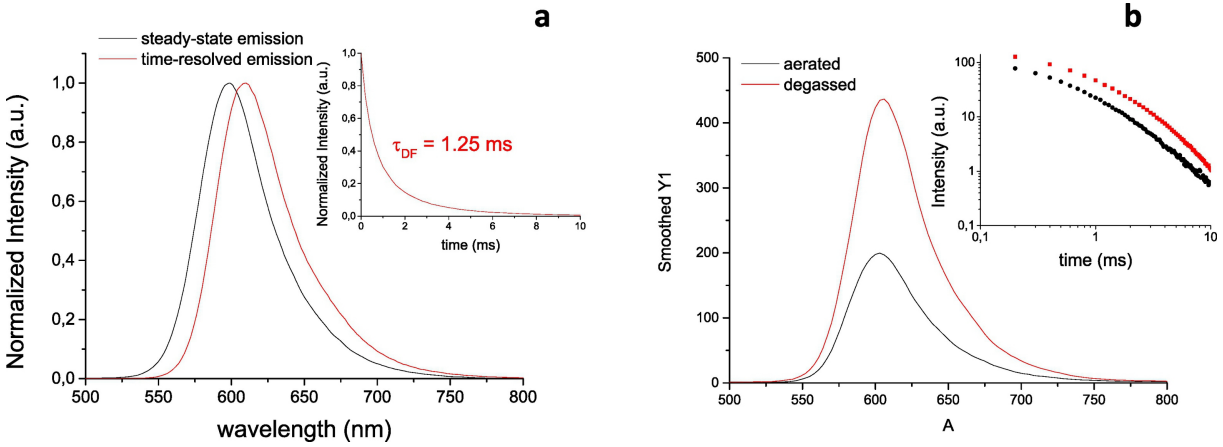
a
steady-state emission
time-resolved emission
Normalized Intensity (a.u.)
wavelength (nm)
Normalized Intensity (a.u.)
time (ms)
τDF = 1.25 ms
b
aerated
degassed
Smoothed Y1
A
Intensity (a.u.)
time (ms)

Figure 5

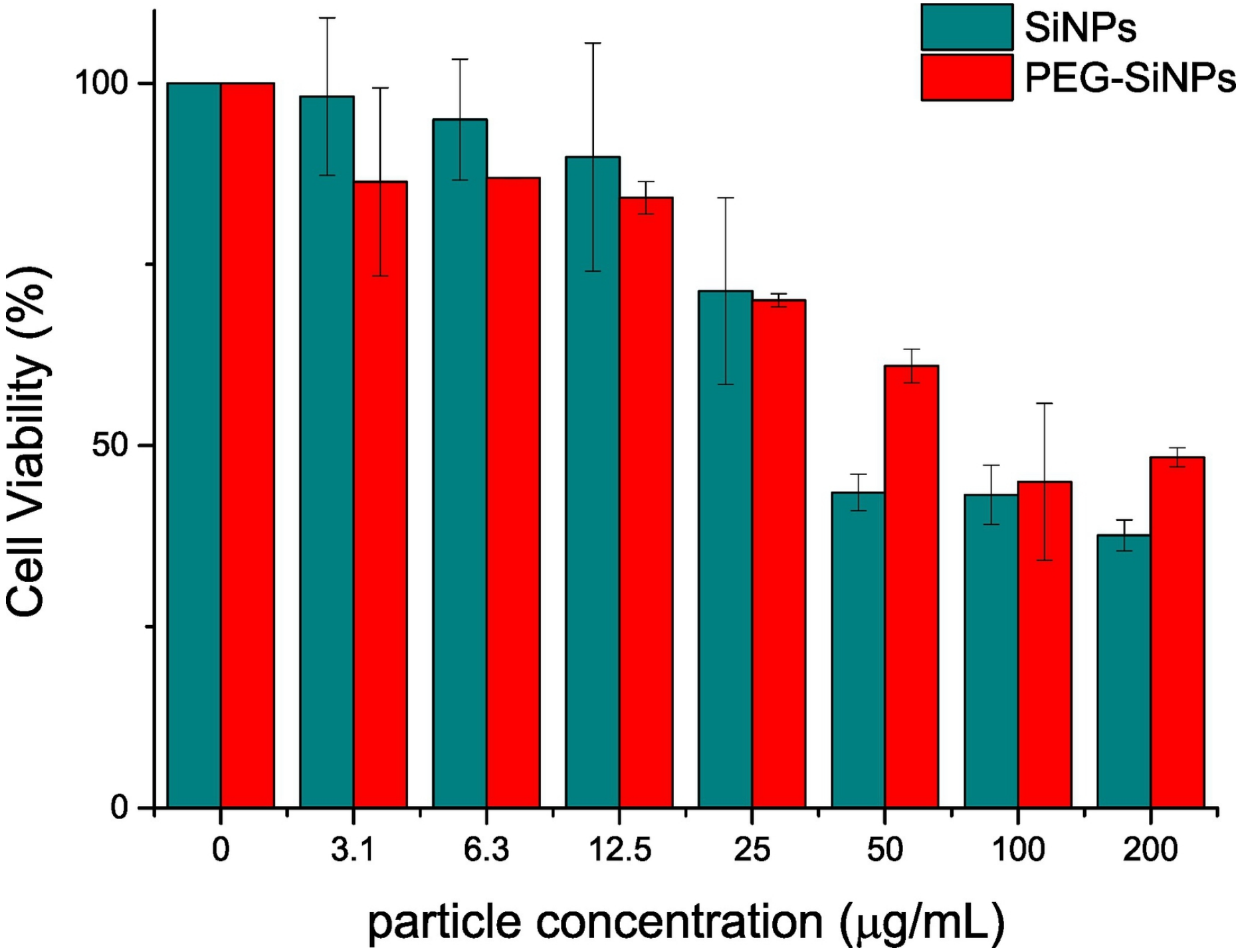
SiNPs
PEG-SiNPs
Cell Viability (%)
100
50
0
0
3.1
6.3
12.5
25
50
100
200
particle concentration (μg/mL)

Figure 6

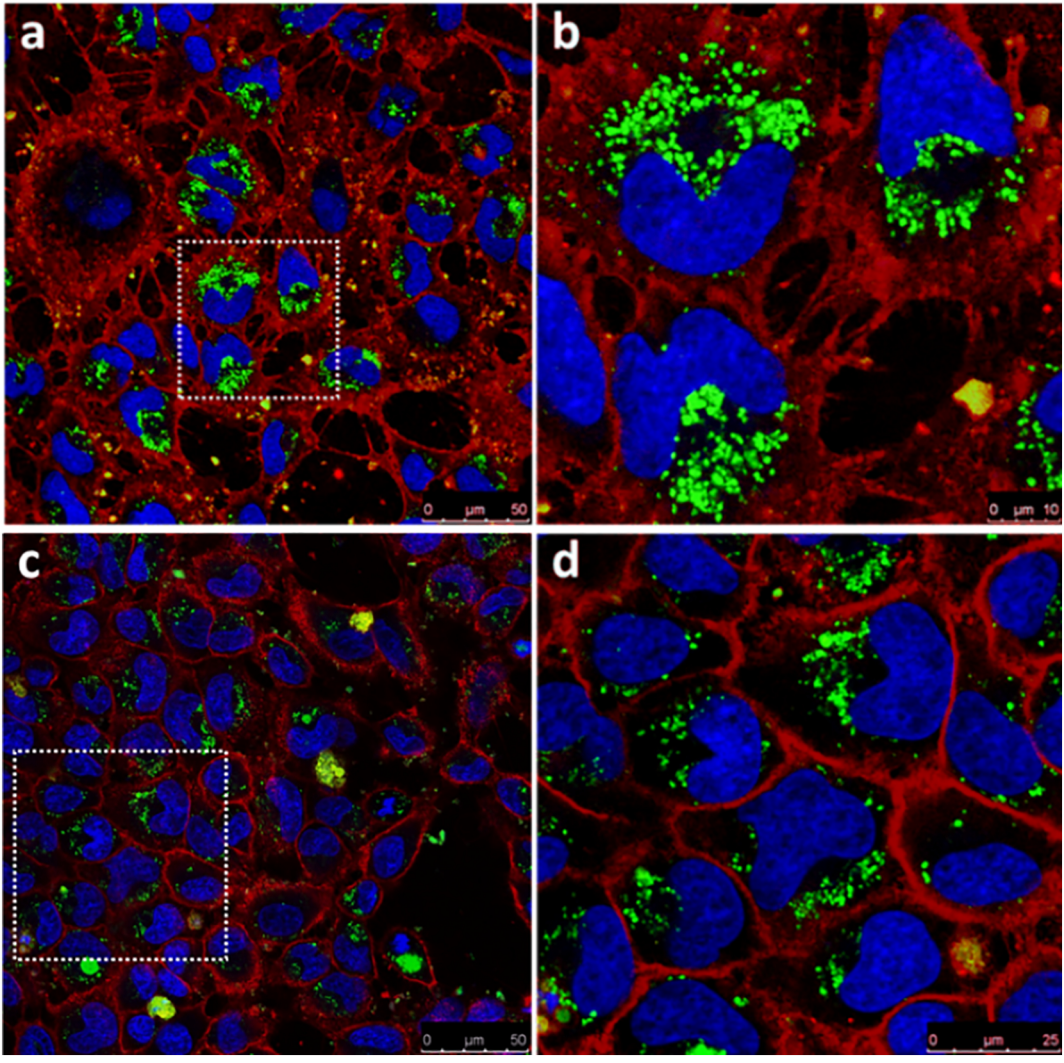

Figure 7

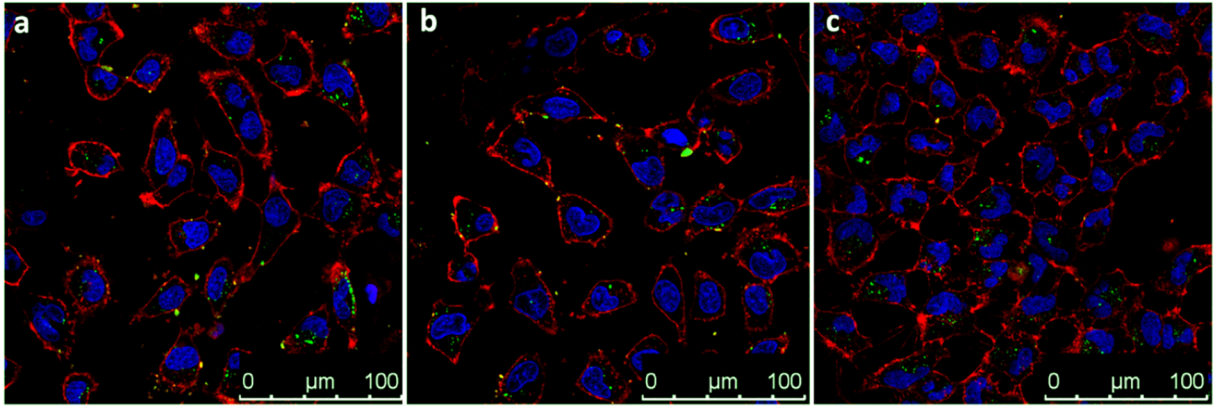

Figure 8

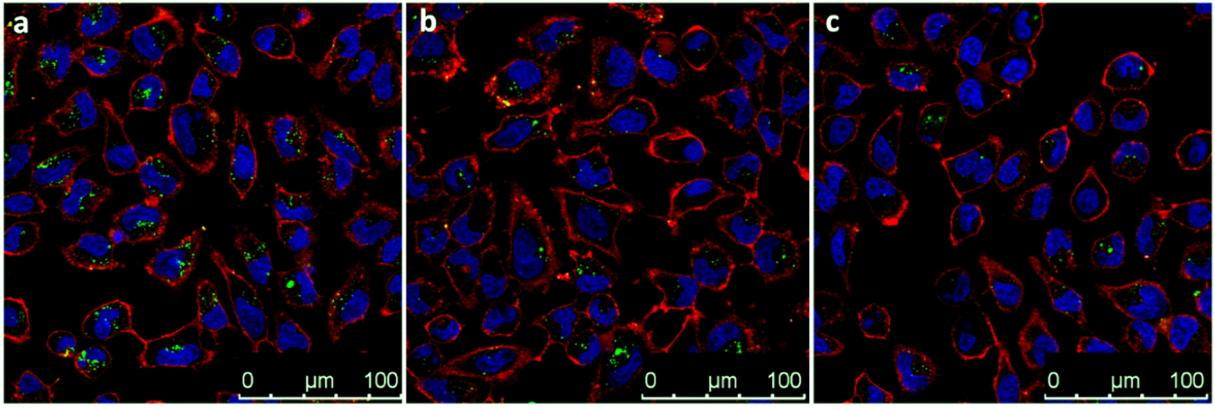

Figure 9